# WIND EFFECTS ON ROOF BALLAST PAVERS

by

B. Bienkiewicz* and R.N. Meroney **

Submitted to

Journal of Structural Division
American Society of Civil Engineering

Fluid Mechanics, Solar, and Wind Engineering Program
Department of Civil Engineering
Colorado State University
Fort Collins, Colorado
80523

* Assistant Professor, ASCE Member
** Professor

Revised September 1986
Revised June 1987
CEP85-86BB-RNM33

# WIND EFFECTS ON ROOF BALLAST PAVERS

by

B.Bienkiewicz and R.N. Meroney

**ABSTRACT:**

Wind blown debris from roofs result in major building damage and failure during severe wind storms. Typically roofs are only 2% of a building cost, but their failure represents about 25% of the hazard related lawsuits. The response of different types of roofing systems to wind loads induced by high wind speeds can be investigated in wind tunnels. This paper reviews fluid model experiments which have identified the primary failure mechanisms of roofs covered by various combinations of single-ply membranes, tiles, pavers, insulation boards and gravels. New data are presented on the uplift performance of pavers with overlap joints, the advantages of paver clips, and the influence of exposure and parapet height on paver movement.

## 1.0 INTRODUCTION:

Roofs are subject to forces of nature such as the sun, wind, rain, snow and hail. The sun can cause ultraviolet damage to the surface; whereas wind, snow and hail can cause loss of containment and permit penetration of rain and cold. In addition roofs must resist the ravages of fire, and accidental puncture, abrasion and vandalism by man. Thus, the ideal roof should be light, fire resistant, ultraviolet light safe, and walkable. It should resist wind-induced failure, and its structure should permit routine inspection.

Man has ingeniously used many surfaces for roofs ranging from earth to ice, but most new, commercial flat-roofed buildings today have built-up roofs (BUR), single-ply-membrane roofs (SPM), modified bitumen roofs (MB), or liquid-applied systems (LAS). Characteristics of metal membrane roofs are not included in this review. Built-up roofs are made from layers of felt, asphalt tar, and stones laid over a support deck. Proponents for other systems claim these traditional

roofs are not cost effective and require the most roof-top work, use expensive oil-asphalt products, split and blister under thermal shock, and require costly double layers of insulation to meet increased insulation standards. Nonetheless, BUR retain 42% of the roofing market [6].

Single-ply roofs now share 34% of the roof market. They are made from prefabricated layers of insulation or insulation boards, a single-ply elastomeric plastic or rubber membrane, and a top ballast of gravel or paving blocks. Still newer, and occupying a 15% market share is the modified bitumen membrane composed of one or more prefab plies of fiberglass or polyester, each ply coated on both sides with a polymer filled bitumen. The MB membranes are affixed to the roof either by torch or hot-applied bitumen. The remaining 9% of the roof market belongs to liquid-applied systems such as polyurethane foams.

Roof ballast materials dislodged during wind storms caused major damage to windows and building cladding during the 1983 Hurricane Alicia in Houston.[9] Although most damage was associated with loose pea gravel from BUR roofs, roofing manufacturers and code officials became concerned about the integrity of all ballasted roofs. Since 1972 wind tunnel experiments have been performed on the behavior of ballasted roofs. The present paper reviews past wind-tunnel experiments reported by various researchers. It also describes a recent wind-tunnel study of a ballasted roof failure conducted by the authors. Section 1.1 reviews the character of ballast on BUR and SPM roofs, section 1.2 reviews the results from previous fluid model experiments. Section 2.0 summarizes similarity requirements for fluid modeling of roof ballast systems; whereas, sections 3.0 and 4.0 report

paver behavior for overlapping and edge clipped pavers under different wind exposures and parapet heights. Incorporation of fluid model results into code statements is provided in section 5.0.

### 1.1 Ballast Characteristics

BUR typically are constructed from crushed rock, slag, or pea gravel about 3/8 inch diameter. Most of this material is adhered together with bitumen. SPM are ballasted with loose stone or gravel no smaller than 3/4 inch or even larger concrete pavers or tiles. SPM manufacturers conventionally lay large insulation boards over a supportive deck. Next, an elastomeric membrane is stretched from roof edge to roof edge, and and then ballast is loose laid over the membrane. Sometimes the membrane is placed beneath the insulation. The membrane is glued or mechanically fastened to the underlying surface, or, alternatively, sealed just at the edges of the roof.

Gravel ballast on SPM roofs are usually round river stones ranging from 1 to 3 in. (25.4 to 76.2 mm) diameter. Crushed stones, slag, or other sharp edges stones are not allowed because of abrasion to the membrane. Gravel ballast typically weighs between 10 to 25 lb/sf (479 to 1198 N/sq m), and layer thickness varies from 1 to 5 in. (25.4 to 127.0 mm). Paving stones are usually square or rectangular pavers cast to provide drainage on the underside. Sometimes they include interlocking edges or other special (usually patented) features. Paver weights range from 11 to 25 lb/sf, and their sizes range from 12 x 12 x 2 in. (0.30 x 0.30 x 0.05 m) to 24 x 24 x 3 in. (0.61 x 0.61 x 0.075 m) and larger. In some cases pavers are prefabricated with insulation bound to the under-side in sizes up to 4 x 8 ft (1.22 x 2.44 m) sheets.

## 1.2 Fluid Modeling Experiments

Wind-tunnel modeling of gravel ballast failures have been performed by Durgin et al. (1972) using lead shot, and by Kind and Wardlaw (1976), Kind (1974, 1977, 1985), and Kramer et al. (1979) using natural gravel.[10,11,12,14,18] They studied gravels with equivalent sizes ranging from 1.5 to 2.8 in. (38 to 75 mm). The upper wind speed limit for gravel to resist scour at building orientations of $45^{o}$ was found to be between 50 to 60 mph (22 to 27 m/s) at a 30 ft (10 m) elevation. Replacing corner regions with ballast pavers in a gravel/paver composite arrangement allowed speeds to increase to over 100 mph (45 m/s) before significant scour occurred. Kind (1985) determined that model gravel as small as 0.004 in.(0.1 mm) can be used in model experiments; thus, useful results are possible from fluid modeling for scale ratios as large as 1:120.[12]

Ballast paver experiments have been performed by Kind et al. (1974, 1982, 1984) and Bienkiewicz and Meroney (1985).[2,10,13,16] Tests included pavers with and without overlapping, pavers with and without taped or fixed joints, parapets of heights varying from 0 to 36 in (0 to 0.91 m), and effects of water pooling. Kind et al. also studied larger insulation boards and membrane behavior under the ballast.

Membrane experiments have been made by Durgin and Allan (1981) and Kramer et al. (1979).[5,18] Durgin and Allan examined lift forces on mechanical tie-downs on an unballasted roof; whereas, Kramer et al. examined the effects of membrane damage on unballasted roofs with suction pressures maintained on the bottom membrane surface.

## 2.0 SIMILITUDE REQUIREMENTS FOR FLUID MODELING OF ROOF BALLAST SYSTEMS

Dimensional analysis and similarity considerations indicate that similitude for fluid modeling of roof ballast systems will be achieved if the wind approaching the model simulates the natural wind, if all model dimensions are correctly scaled, and if the Reynolds number, $UL/\nu$; the Froude number, $U^2/gL$; and density ratios of air and ballast materials have the same numerical values in both the model and prototype situations. It is impossible to match both the Reynolds and Froude numbers in a fluid model experiment, but fortunately it is well established that flows over sharp edged building shapes are independent of Reynolds numbers for moderately high wind speeds.

In the case of thin objects such as insulation boards or pavers scaling of the density ratio can be relaxed and replaced by the similarity requirement that the weight per unit area ratios be the same for model and prototype, or $(\sigma t)_m/(\sigma t)_p = L_m/L_p$, where $\sigma$ is paver density, t denotes paver thickness, and the subscripts m and p denote model and prototype respectively. The adjustment of model paver thickness and density permits the use of convenient modeling materials to represent both the prototype concrete paver and/or foam insulation boards.

The remaining similarity requirement--the Froude number--is satisfied when the wind speed scale, $\lambda_V$, and the geometrical scale, $\lambda_L$, are related as:

$$\lambda_V = (U_m/U_p) = \lambda_L^{1/2} = (L_m/L_p)^{1/2}.$$

This relation can be used to compute the prototype wind speed corresponding to a given wind tunnel speed.

## 3.0 WIND EFFECTS ON ROOF BALLAST SYSTEMS

Wind accelerating over a roof top produces low pressure patterns which can combine with internal building pressues to produce a net local uplift on a roof element. Roof pressures are a function of building height, exposure, building orientation, parapet heights, and other roof top features such as elevator housings, stairwell covers, and cooling towers. Very little full scale information is available on roof pressures; hence, the flow situation is understood primarily from wind-tunnel measurements.[3,8,12,17,20].

### 3.1 Features of the Roof Pressure Field

Maximum negative values of pressure coefficient, $Cp = (p-p_o)/(\rho U^2/2)$, occur for a rectangular building when its corners are alligned at a $45^o$ angle to the approach wind. In this case twin vortex "tornadoes" form which produce minimum pressures near the building edges in the region of the upwind corner. Minimum mean Cp values lie between -3 and -4 for an unparapeted building. Ballast movement actually occurs as a result of short period gusts which exceed the mean wind speed, and consequently produce local maximums in lift pressure. Very little information is available about such pressure fluctuations, their size, their persistence, and how they relate to the gusty approach wind. First expectations might be that a building parapet should increase sheltering and reduce roof loads. Wind-tunnel measurements made by Stathopoulos (1982), and Stathopoulos and Baskaran (1985) suggest that small parapets may, in fact, actually increase roof loads over pavers substantially.[19,20] In general parapets do reduce the maximum suction on the roof edges, but they slightly increase the magnitude of suction on the interior areas of

the roof. Yet roof corner suctions actually increase significantly for low parapet heights [0 to 6 in. (0 to 152 mm)], and low parapets spread suction minimums over larger areas; thus increasing the likelihood that uplift exceeds paver or ballast weight. As parapet height increases true sheltering occurs, and the region where ballast uplift occurs moves downwind from the corner.

### 3.2 Response of Ballast to Pressure Fields

Ballast gravel is usually blown toward low pressure regions and away from the corner diagonal. Once the ballast is removed from the single-ply membrane, it may balloon, ripple, or tear. Often the gravel accumulates against the back face of the upwind parapet, or the gravel is actuallly caught up into the low pressure regions and catapulted off the roof.

For loose laid ballast systems the pressure field communicates to regions beneath the pavers by means of the cracks between the ballast. The region beneath the paver responds almost instantaneously to changes in pressure above; however, the pressure tends to vary linearly between the joints. Since the pressure above the paver can have a minimum over mid-paver, the result is a net up-lift. This pressure difference can become large enough to lift the ballast materials off the roof.

Initial failure of roof pavers occurs about four feet downwind of the corner next to the parapet wall. The paver rotates about its roof-edge side, moves upwind, and then tumbles downwind in the windflow coming over the building edge. Once one paver is missing the remaining pavers shuffle into the low pressure region and also displace toward the parapet. If one edge of the paver is interlocked

beneath another block on the edge away from the wall, then the paver resists movement at lower wind speeds, and it is finally dislodged at much higher wind speeds.

### 3.3 Wind-tunnel Experiments on Interlocking and Edge Clipped Ballast Pavers

The performance of interlocking pavers and pavers with edge clips was evaluated during a wind-tunnel study conducted at the Fluid Dynamics and Diffusion Laboratory, Colorado State University. The study was conducted in the Industrial Aerodynamics Wind Tunnel, which is of recirculating type with a test section 6 x 6 ft (2 x 2 m) and 60 ft long (18 m). Model blockage effects can be resolved with an adjustable test-section ceiling. Simulated atmospheric boundary conditions are created by placing flow modifying spires at the entrance to the test section and a uniform fetch of roughness elements on the floor upwind of the model.

Model Building and Pavers - Model pavers were placed in various configurations on a roof of a model building chosen to simulate flow conditions on a typical flat roof. Detailed pressure measurements were not made during this study. The pattern of pressure is not expected to differ significantly from those presented by other authors[16,20,21]. No model membrane was installed beneath the model pavers. Membrane thickness, elasticity, and hold-down features vary significantly from manufacturer to manufacturer. These tests may be conservatively interpreted as representative of tile failure when the membrane is glued or firmly attached to the underlying support structure. Thus, it is presumed membrane ballooning does not participate in or initiate tile movement. The building model with a

typical parapet and model pavers is shown in Figures 1 and 2. The model at a scale of 1:15 represented a 15 ft (4.6 m) tall prototype building with a 22 ft square (6.7 m) flat roof. A large model scale was selected to permit the use of larger size model pavers. The size of the model was limited by the size of the wind-tunnel test section, and by the desire to maintain blockage below 5%. The model was configured with parapets of various heights. Model ballast pavers were made of plexiglass and dimensioned as noted in Figure 1b. An equivalent full scale paver which weighed 11 1/2 lb/sf (570 N/sq m) would have dimensions of 11 3/4 x 16 1/2 x 1 5/16 in. (0.358 x 0.419 x 0.033 m).

All experiments were performed for the critical $45^{o}$ building orrientation. Kind and Wardlaw (1982) indicated that the roof flow field is mainly dependent on the speed of the approaching wind at rooftop level.[16.] It was assumed that characteristics of the rooftop flow were only minimally dependent on building height to boundary layer depth ratio. A series of pretests performed over a zero-height-parapet building revealed that ballast movement correlated with rooftop wind speed for powerlaw exponents ranging from 0.1 to 0.3.

Pavers were arranged in a configuration shown in Figure 3a. A modified configuration of the pavers was also investigated to evaluate the effects of paver staggering. The pavers were arranged in a staggered pattern as noted in Figure 3b. The outer pavers along one roof edge were connected together by circular adhesive paper tabs attached to the upper and lower surfaces of the two adjacent pavers to simulate the presence of mechanical metal clips attached between

pavers in high-uplift regions.

Flow Conditions - Two representative approach flow configurations were simulated. One of the configurations represented conditions typical for flow over open or rural country (Uniform Building Code - Exposure C, ANSI A58.1-1982 - Exposure C). The other situation modeled flow over built-up or uban terrain (Uniform Building Code - Exposure A, ANSI A58.1-1982 - Exposure A).[1,7] Based on scale lengths of roughness length, $z_o$, integral scale, $\Lambda_x$, and atmospheric boundary laer thickness, $\delta$, the geometric scale of the modeled boundary layer ranges between 1:200 to 1:300 [2]. Fortunately the geometric scale of the model and the slope of the approaching velocity profile should be only of secondary imprtance, because it appears that the wind speed at rooftop level is the dominant factor as regards tile movement[11]. Meroney (1986) reviewed data from 23 wind-tunnel studies of pressure measurements over prismatic building shapes. He found that minimum roof pressure coefficients were most sensitive to rooftop turbulence intensity magnitude and not as sensitive to roof height to boundary layer thickness ratio. No systematic variation in minimum pressure coefficients occured if roof height to boundary layer thickness ratio was between 0.2 to 1.0. When turbulence intensities at building height exceed 15%, pressures do become more negative. Moreover, for roof orientations of $45^o$ the minimum roof pressures varies only slightly with such parameters [19].

The turbulent boundary layer generated by the spires, barrier and surface roughness was about 40 in. (1.0 m) deep at the model location. Figure 4 depicts the mean velocity and turbulent intensity profiles achieved at that location. Such velocity profiles are frequently

described by an empirical power-law relationship, $U/U_{ref} = (z/z_{ref})^{\alpha}$. The model power law coefficients, $\alpha$, for the two cases tested were 0.14 and 0.37 for Exposures C and A, respectively.

Test Procedure - During the wind-tunnel experiments the pavers were placed on the roof of the building model in a desired arrangement. Wind speed in the tunnel was gradually increased, and the behavior of the pavers was observed. Wind speed was measured by a pitot-static tube mounted at rooftop level of the model building. When a paver failure (dislocation) was observed, the wind-tunnel speed was recorded. The prototype wind speed, corresponding to the measured mean wind speed at paver failure was called the failure wind speed at roof height, and it was denoted by $V_D$. The paver failure wind speed, $V_D$, was averaged over several separate replications of each flow condition, paver configuration, and parapet height. It should be noted that since the wind speed approaching the building model is turbulent, the paver failure is a random event initiated by peak velocities (greater than the mean), which are of sufficient spatial distribution and temporal duration to cause the paver or pavers to uplift.

## 4.0 RESULTS FROM FLUID MODEL EXPERIMENTS

The paver failure wind speed is summarized in Table 1 for two paver configurations, three wind exposures, and five parapet heights. The failure wind speed depends on the paver configuration. It is higher for the modified configuration (staggered pavers with edge clips) than for the original configuration (unstaggered pavers without edge clips) The difference between the failure wind speed for the two configurations decreases as the parapet height increases. For parapet

heights above 18 in. (0.46 m) failure wind speeds have the same magnitude for the two configurations; however, it is entirely possible that the building depth to parapet height has become the limiting factor in the experiments.

### 4.1 Failure Mode of Ballast Pavers - Original Configuration

Failure wind speed at rooftop is plotted in Figure 5 as a function of the parapet height. The failure wind speed is higher for Exposure C than Exposure A. This suggests that an increase in turbulence level results in a decrease in the mean wind speed associated with the paver failure. The effects of the parapet height are similar for both exposure conditions. A relatively low height parapet (up to about 6 in.) causes a decrease in the failure wind speed, $V_D$; whereas a parapet of greater height results in an increase in the failure wind speed. The failure mode of the pavers is very consistent. Failure was initiated when one or two pavers located in positions 1,4 or 1,5 as shown in Figure 6 dislodged. Then nearby pavers shuffled or vibrated sideways into this region, rotated toward the parapet and also dislodged. Eventually a large number of pavers in the roughly triangular region downwind from these positions also failed.

### 4.2 Failure Mode of Ballast Pavers - Staggered and Edge Clipped

Failure wind speed at rooftop for the modified configuration is plotted in Figure 7 as a function of the parapet height. Paver failure occured at higher wind speed for the modified configuration. The character of the failure of the pavers arranged in the modified configuration also differed from the original configuration. Failure

initiated near positions (1,4) or (1,5), but the failure was more sudden, and more pavers were dislodged simultaneously. As noted in Figure 8, sometimes almost half of the roof tiles failed together after the edge clipped pavers buckled and displaced.

## 5.0 DESIGN CONSIDERATIONS FOR BALLAST INSTALLATION

The mean wind speed at the rooftop level at which paver failure occurs or failure wind speed, $V_D$, can be used to establish rough design criteria for the use of ballast pavers on roofs of typical low-rise buildings located within uniform surroundings as defined in codes and standards. The basic wind speed, $V_m$, is specified by codes and standards as the fastest mile wind speed at a height of 30 ft (10 m) above the ground. The peak wind speed used in design, $V_H$, at rooftop height H is approximately related to the basic wind speed by

$$V_H = C_H V_m, \qquad \text{Eq (1)}$$

where $C_H$ is a correction factor for variation in the wind speed and gustiness with height. It is proposed that a conservative condition for the paver failure for a building of height H would be $V_H = V_D$, ie. during paver failure the expected peak velocity at rooftop would be assumed equal to the failure wind speed established during the wind-tunnel study. Since the ratio $V_H/V_D$ may be expected to be greater than 1.30, the approach invoves a reasonable level margin of safety.

### 5.1 Design Considerations Using Uniform Building Code

The Uniform Building Code recommends a coefficient, $C_e(z)$, to correct for combined effects of height , exposure, and gust factor (Table No. 23-G, UBC (1982)).[7] This factor may be approximated by the expressions,

Exposure C:

$$C_e(z) = \begin{cases} -1.11\text{x}10^{-5}\ z^2 + 6.33\text{x}10^{-3}\ z + 1.078, & z \leq 120 \text{ ft} \\ 1.433 + 2.22\text{x}10^{-3}\ z, & z > 120 \text{ ft} \end{cases}$$

Exposure B:

$$C_e(z) = \begin{cases} -1.11\text{x}10^{-5}\ z^2 + 6.33\text{x}10^{-3}\ z + 0.558, & z \leq 120 \text{ ft} \\ 0.983 + 2.22\text{x}10^{-3}\ z, & z > 120 \text{ ft.} \end{cases}$$

Given that $C_e(H) \cong C_H^2$, then the maximum permissible building height, H, can be calculated from Equation (1) for any exposure, design wind speed, and parapet height from Figures 5 or 7 for the paver geometries studied. Table 2 presents the result of such calculations for the UBC code. Situations resulting in building heights less than 10 ft high have been set to zero height.

**5.2 Design Considerations Using ANSI Standard A58.1-1982.**

The paver failure condition can be written in terms of the wind/load parameters specified by ANSI as $C_H^2 = K_z(H)\ G_z(H)$, where $K_z$ is a pressure exposure coefficient and $G_z$ is a gust response factor.[1] The pressure coefficient and the gust response factor are defined by ANSI as

$$K_z = \begin{cases} 2.58(z/z_g)^{2/\alpha}, & \text{for } z \geq 15 \text{ ft} \\ 2.58(15/z_g)^{2/\alpha}, & \text{for } z < 15 \text{ ft} \end{cases}$$

and

$$G_z = 0.65 + 0.35\ T_z,$$

where

$z$ = height (ft),

$z_g$ = gradient wind height (ft),

$\alpha$ = velocity power law coefficient,

$T_z = 2.35\ D_o^{1/2}/(z/30)^{1/\alpha}$, and

$D_o$ = surface drag coefficient.

The gradient height, $z_g$, the power law coefficient, , and the surface drag coefficient, $D_o$, are specified by ANSI and summarized in Table 3. The numerical values computed for maximum permissible building height, H, are summarized in Table 4 for two paver configurations, three wind exposures, five parapet heights, and different values of the basic wind speed.

### 5.3 Comparison of Results Obtained from UBC and ANSI Codes

The maximum building height for a 12 inch parapet computed using UBC (Section 5.1) and ANSI (Section 5.2) is compared for the wind exposures C and B in Figures 9 and 10 for the original and modified paver configurations. Maximum building heights, computed using the two approaches, are similar for the wind Exposure C, but the use of the UBC code leads to more conservative results for the wind Exposure B. The present study confirms observations made by Kind and Wardlaw (1979, 1982) that failure wind speed is dependent on wind exposure and associated turbulence intensity, parapet height, paver orrientation, and the presence of paver interlocks.[15,16]

## 6.0 CONCLUSIONS

The results of this study indicate that wind effects on and failure of ballast pavers are of a complicated nature; nonetheless, several observations and conclusions can be provided:

a. The failure wind speed at rooftop is affected by wind exposure and parapet height.
b. As the level of turbulence in the approach wind increases, the failure wind speed decreases.
c. Low height parapets cause a reduction in the failure wind speed when compared with the failure speed for the zero

height parapet.

d. Moderate height parapetes result in an increase in the failure wind speed.
e. Failure wind speeds are higher for staggered and edge clipped pavers than for unstaggered pavers without edge clips.
f. Paver height and exposure affect the two paver configurations similarly.
g. The design methodology proposed results in conservative values for the maximum heights of buildings employing similar prototype pavers installed in similar wind field environments.
h. The results of this study are in agreement with the results of studies performed by other researchers.

**REFERENCES:**


1. American National Standards Institute (1982), Minimum Design Loads for Buildings and Other Structures, ANSI A58.1-1982, New York, NY.

2. Bienkiewicz, B. and R.N. Meroney (1985), "Wind-Tunnel Study of Westile Ballast Paver," Civil Engineering Report CER85-86BB-RNM13, Colorado State University, Fort Collins, CO, 98 pp.

3. Chien, N.; Feng, Y.; Wang, H.; and Siao, T.T. (1951), "Wind Tunnel Studies of Pressure Distribution on Elementary Building Forms," Iowa Institute of Hydraulic Research, State University of Iowa, Iowa City.

4. Durgin, F.H., O'Neill, T.O., and Debout, B. (1972) ROOF LIFT OFF TESTS OF THE TROCAL ROOF SYSTEM FOR DYNAMIT NOBEL OF AMERICA, Wright Brothers Wind Tunnel TR 1062, Mass. Inst of Technology, Cambridge, 45 pp.

5. Durgin, F.H., and Allan, J. (1981), A WIND TUNNEL STUDY OF THE PRESSURE AND TIE-DOWN LOAD ON A TYPICAL MEMBRANE ROOF, Wright Brothers Memorial Wind Tunnel WBWT-TR-1135, Mass. Inst. of Technology, Cambridge, 83 pp.

6. Godfrey, K.A. (1986), "ROOF MEMBRANES: New Systems, New Problems," Civil Enginering/ASCE, Vol. , pp. 76-79.

7. International Conference of Building Officials (1982), Uniform Building Code, Whitttier, CA.

8. Jensen, M. and Franck, N. (1963), Model-Scale Tests in Turbulent Wind, Part I: Phenomena Dependent on the Wind Speed, Danish Technical Press, Copenhagen, 97 pp.

9. Kareem, A. (ed.) (1984), "Hurricane Alicia: One Year Later, Proceedings of", ASCE, Galveston, Texas, 16-17 August, 1984, 335 pp.

10. Kind, R.J. (1974), WIND TUNNEL TESTS ON SOME BUILDING MODELS TO MEASURE WIND SPEEDS AT WHICH GRAVEL IS BLOWN OFF ROOFTOPS, National Research Council Canada, National Aeronautical Establishment, Ottawa, LTR-LA-162, 32 pp.

11. Kind, R.J. (1977), FURTHER WIND TUNNEL TESTS ON BUILDING MODELS TO MEASURE WIND SPEEDS AT WHICH GRAVEL IS BLOW OFF ROOFTOPS, National Research Council Canada, National Aeronautical Establishment, Ottawa, LTR-LA-189, 17 pp.

12. Kind, R.J. (1985), MEASUREMENT IN SMALL WIND TUNNELS OF WIND SPEEDS FOR GRAVEL SCOUR AND BLOWOFF FROM ROOFTOPS, Proceedings of 6th Colloquium on Industrial Aerondynamics, Aachen, BRD, June 1985, pp. 197-212

13. Kind, R.J. Savage, M.G., and Wardlaw, R.L. (1984), FURTHER MODEL STUDIES OF THE WIND RESISTANCE OF TWO LOOSE-LAID ROOF-INSULATION SYSTEMS (HIGH-RISE BUILDINGS), National Research Council Canada, National Aeronautical Establishment, Ottawa, LTR-LA-269, 57 pp.

14. Kind, R.J. and Wardlaw, R.L. (1976), DESIGN OF ROOFTOPS AGAINST GRAVEL BLOW-OFF, National Resarch Council Canada, National Aeronautical Establishment, Ottawa, NRC No. 15544, 33 pp.

15. Kind, R.J. and Wardlaw, R.L. (1979), MODEL STUDIES OF THE WIND RESISTANCE OF TWO LOOSE-LAID ROOF-INSULATION SYSTEMS, National Research Council Canada, Natioanl Aeronautical Establishment, Ottawa, LTR-LA-234, 47 pp.

16. Kind, R.J. and Wardlaw, R.L. (1982), FAILURE MECHANISMS OF LOOSE-LAID ROOF-INSULATION SYSTEMS, Journal of Wind Engineering and Industrial Aerodynamics, Vol. **9**, pp. 325-341

17. Kramer, C. (1985), WIND EFFECTS ON ROOFS AND ROOF COVERINGS, Proceedings of the 5th U.S. National Conference on Wind Engineering, 6-8 November 1985, Lubbock, Texas, pp. 17-33

18. Kramer, C., Gerhardt, H.J., and Kuster, H.W. (1979), ON THE WIND-LOADING MECHANISM OF ROOFING ELEMENTS, Journal of Industrial Aerodynamics, Vol. **4**, pp. 415-427.

19. Meroney, R.N. (1986), "WIND-TUNNEL MODELING OF FLOW OVER BLUFF BODIES", Sonderfarchungsbereich 210 fur Bauwerke, University of Karlsruhe, or Colorado State University, CE Memorandum 86-87RNM-48

20. Stathopoulos, T. (1982), WIND PRESSURES ON LOW BUILDINGS WITH PARAPETS, Journal of the Structural Division, ASCE, Vol. **108**, ST12, pp. 2723-2736

21. Stathopoulos, T. and Baskaran, A. (1985), THE EFFECTS OF PARAPETS ON WIND-INDUCED ROOF PRESSURE COEFFICIENTS, Proceedings of the 5th U.S. National Conference on Wind Engineering, 6-8 November 1985, Lubbock, Texas, pp. 3A-29 to 3A-36

**LIST OF FIGURES:**



**LIST OF TABLES:**

Table 1. Failure Wind Speed at Roof Height

ORIGINAL CONFIGURATION

| Wind Exposure | Parapet Height (in.) 0 | 2 | 6 | 12 | 18 |
|---|---|---|---|---|---|
| A‡ | 70 | 65.7 | 66 | 82.1 | 108.4 |
| B‡‡ | 72 | 67.9 | 67.7 | 87.9 | 122.2 |
| C‡ | 74 | 70 | 69.3 | 93.6 | 136 |

MODIFIED CONFIGURATION

| Wind Exposure | Parapet Height (in.) 0 | 2 | 6 | 12 | 18 |
|---|---|---|---|---|---|
| A‡ | 98.9 | 88.2 | 82.4 | 87.2 | 101.2 |
| B‡‡ | 107.4 | 96.3 | 93.1 | 100.8 | 117.6 |
| C‡ | 115.8 | 104.3 | 103.7 | 114.4 | 133.9 |

‡ Measured in Wind Tunnel

‡‡ Interpolated between values for Exposures A and C

Table 2a. Maximum Building Height (ft) Estimated Using UBC -- Modified Configuration, Exposure C and B

| Exposure | C | | | | | B | | | | |
|---|---|---|---|---|---|---|---|---|---|---|
| Basic Wind Speed | Parapet Height (in.) | | | | | Parapet Height (in.) | | | | |
| Um (mph) | 0 | 2 | 6 | 12 | 18 | 0 | 2 | 6 | 12 | 18 |
| 60 | 1032 | 716 | 700 | 992 | 1598 | 1235 | 918 | 903 | 1195 | 1801 |
| 70 | 587 | 355 | 343 | 558 | 1003 | 790 | 557 | 546 | 760 | 1205 |
| 80 | 298 | 126 | 121 | 276 | 616 | 501 | 66 | 48 | 97 | 819 |
| 90 | 114 | 45 | 43 | 104 | 352 | 61 | 11 | 0 | 29 | 554 |
| 100 | 45 | 0 | 0 | 39 | 155 | 12 | 0 | 0 | 0 | 53 |
| 110 | 0 | 0 | 0 | 0 | 73 | 0 | 0 | 0 | 0 | 10 |
| 120 | 0 | 0 | 0 | 0 | 28 | 0 | 0 | 0 | 0 | 0 |

Table 2b. Maximum Building Height (ft) Estimated Using UBC -- Original Configuration, Exposure C and B

| Exposure | C | | | | | B | | | | |
|---|---|---|---|---|---|---|---|---|---|---|
| Basic Wind Speed | Parapet Height (in.) | | | | | Parapet Height (in.) | | | | |
| Um (mph) | 0 | 2 | 6 | 12 | 18 | 0 | 2 | 6 | 12 | 18 |
| 60 | 82 | 49 | 44 | 451 | 1669 | 64 | 34 | 33 | 653 | 1872 |
| 70 | 0 | 0 | 0 | 160 | 1055 | 0 | 0 | 0 | 94 | 1258 |
| 80 | 0 | 0 | 0 | 50 | 656 | 0 | 0 | 0 | 21 | 859 |
| 90 | 0 | 0 | 0 | 0 | 383 | 0 | 0 | 0 | 0 | 586 |
| 100 | 0 | 0 | 0 | 0 | 177 | 0 | 0 | 0 | 0 | 76 |
| 110 | 0 | 0 | 0 | 0 | 83 | 0 | 0 | 0 | 0 | 26 |
| 120 | 0 | 0 | 0 | 0 | 35 | 0 | 0 | 0 | 0 | 0 |

Table 3. Wind Exposure Characteristics Specified by ANSI Standard

| Exposure | Power Law Exponent n | Gradient Height $z_g$ (ft) | Surface Drag Coefficient $D_o$ |
|---|---|---|---|
| A | 3 | 1500 | 0.025 |
| B | 4.5 | 1200 | 0.010 |
| C | 7 | 900 | 0.005 |
| D | 10 | 700 | 0.003 |

$$n = \frac{1}{\alpha}$$

Table 4a. Maximum Building Height (ft) Estimated Using ANSI Standard -- Original Configuration, Exposure A, B and C

| Exposure | C | | | | | B | | | | | A | | | | |
|---|---|---|---|---|---|---|---|---|---|---|---|---|---|---|---|
| Basic Wind Speed | Parapet Height (in.) | | | | | Parapet Height (in.) | | | | | Parapet Height (in.) | | | | |
| Um (mph) | 0 | 2 | 6 | 12 | 18 | 0 | 2 | 6 | 12 | 18 | 0 | 2 | 6 | 12 | 18 |
| 60 | 82 | 50 | 45 | 651 | 14809 | 216 | 153 | 150 | 677 | 4092 | 489 | 389 | 385 | 1044 | 3446 |
| 70 | 20 | 12 | 11 | 169 | 4172 | 86 | 60 | 59 | 281 | 1786 | 267 | 210 | 208 | 583 | 1987 |
| 80 | 0 | 0 | 0 | 51 | 1359 | 38 | 26 | 26 | 128 | 856 | 155 | 121 | 120 | 347 | 1220 |
| 90 | 0 | 0 | 0 | 17 | 495 | 18 | 12 | 12 | 63 | 441 | 95 | 74 | 73 | 216 | 785 |
| 100 | 0 | 0 | 0 | 6 | 197 | 0 | 0 | 0 | 33 | 240 | 60 | 46 | 46 | 140 | 525 |
| 110 | 0 | 0 | 0 | 3 | 84 | 0 | 0 | 0 | 18 | 137 | 39 | 30 | 30 | 94 | 362 |
| 120 | 0 | 0 | 0 | 1 | 38 | 0 | 0 | 0 | 10 | 81 | 27 | 20 | 20 | 65 | 256 |

Table 4b. Maximum Building Height (ft) Estimated Using ANSI Standard -- Modified Configuration, Exposure A, B and C

| Exposure | C | | | | | B | | | | | A | | | | |
|---|---|---|---|---|---|---|---|---|---|---|---|---|---|---|---|
| Basic Wind Speed | Parapet Height (in.) | | | | | Parapet Height (in.) | | | | | Parapet Height (in.) | | | | |
| Um (mph) | 0 | 2 | 6 | 12 | 18 | 0 | 2 | 6 | 12 | 18 | 0 | 2 | 6 | 12 | 18 |
| 60 | 3947 | 1641 | 1563 | 3567 | 13047 | 2046 | 1126 | 934 | 1448 | 3335 | 2175 | 1463 | 1292 | 1729 | 3008 |
| 70 | 1077 | 438 | 416 | 971 | 3665 | 877 | 475 | 391 | 615 | 1448 | 1240 | 825 | 726 | 979 | 1729 |
| 80 | 340 | 135 | 128 | 306 | 1190 | 413 | 220 | 180 | 287 | 690 | 752 | 495 | 434 | 591 | 1058 |
| 90 | 120 | 47 | 44 | 108 | 432 | 209 | 110 | 89 | 144 | 354 | 479 | 312 | 273 | 374 | 679 |
| 100 | 46 | 18 | 17 | 41 | 171 | 112 | 58 | 47 | 76 | 192 | 317 | 204 | 178 | 246 | 452 |
| 110 | 19 | 0 | 0 | 17 | 73 | 63 | 32 | 26 | 43 | 109 | 216 | 138 | 120 | 167 | 311 |
| 120 | 0 | 0 | 0 | 0 | 33 | 37 | 18 | 15 | 25 | 64 | 151 | 96 | 83 | 116 | 219 |

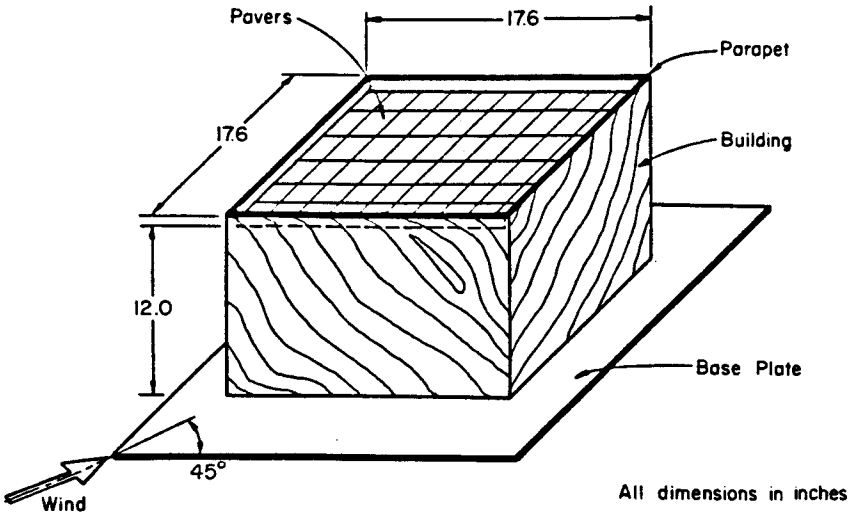


Paver Model

Figure 1a. Building Model

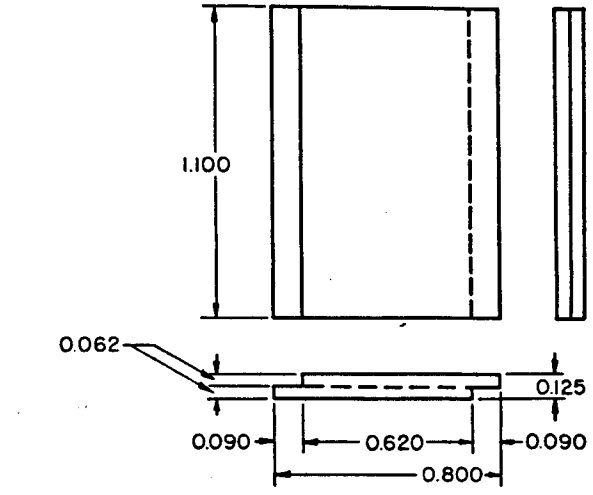


Figure 1b. Paver Model

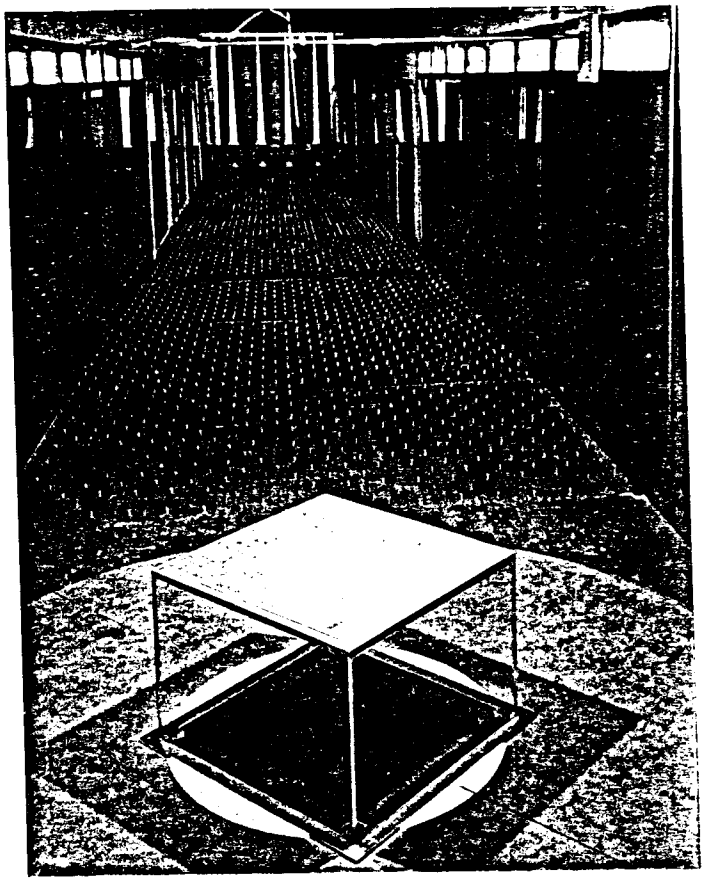

Figure 2. Boundary Layer Generators and Model Building

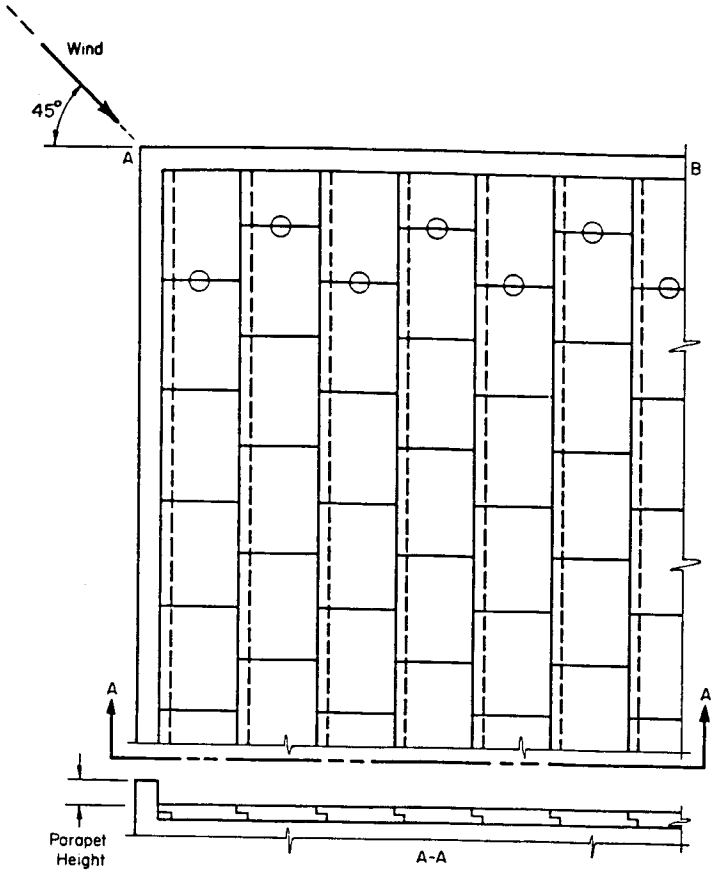


Figure 3b. Details of Paver Layout - Modified Configuration

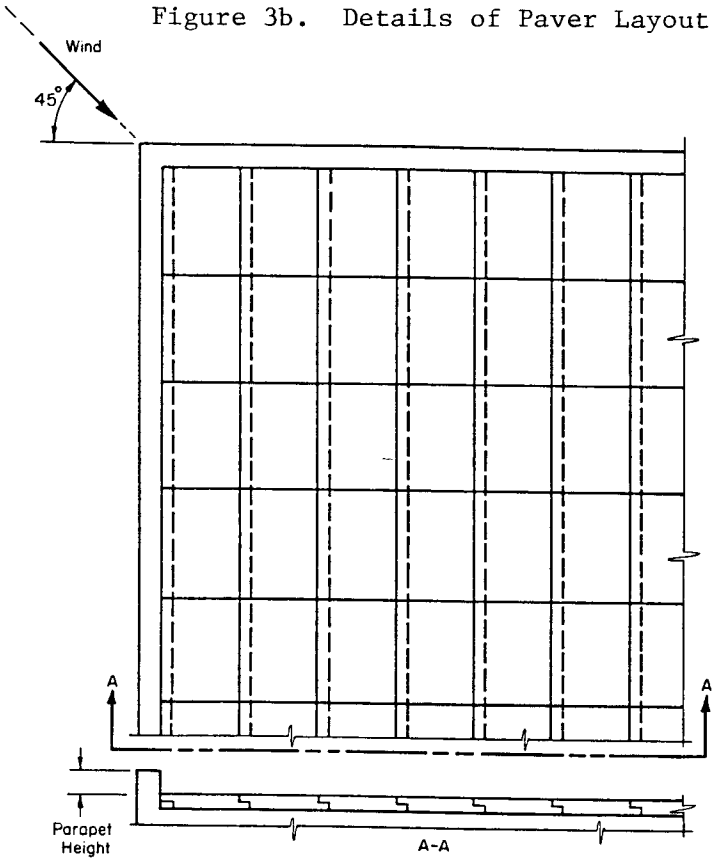


Figure 3a. Details of Paver Layout -- Original Configuration

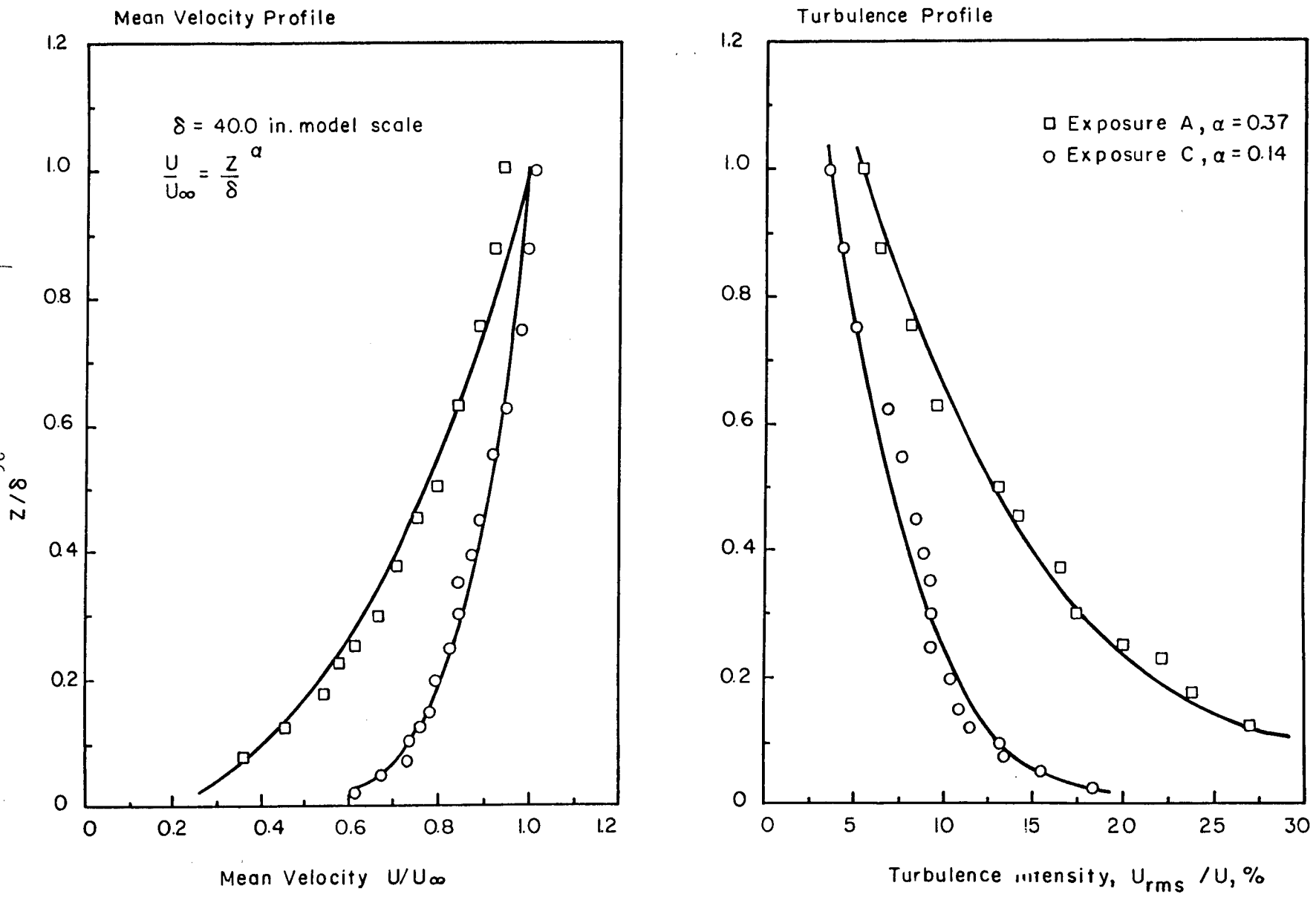


Figure 4. Mean Wind Speed and Turbulence Intensity Profiles -- Exposure A & C.

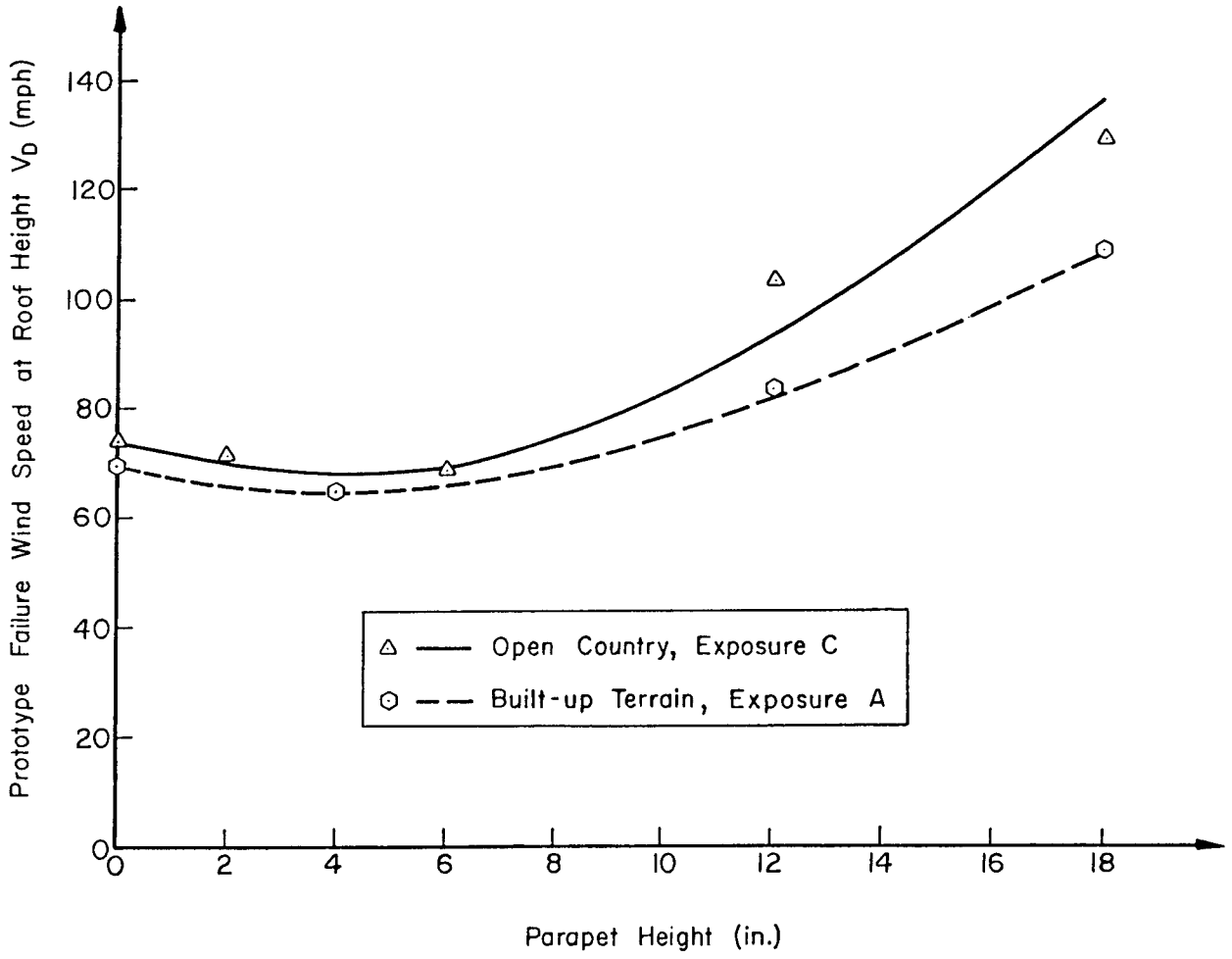


Figure 5. Failure Wind Speed at Roof Height -- Original Configuration

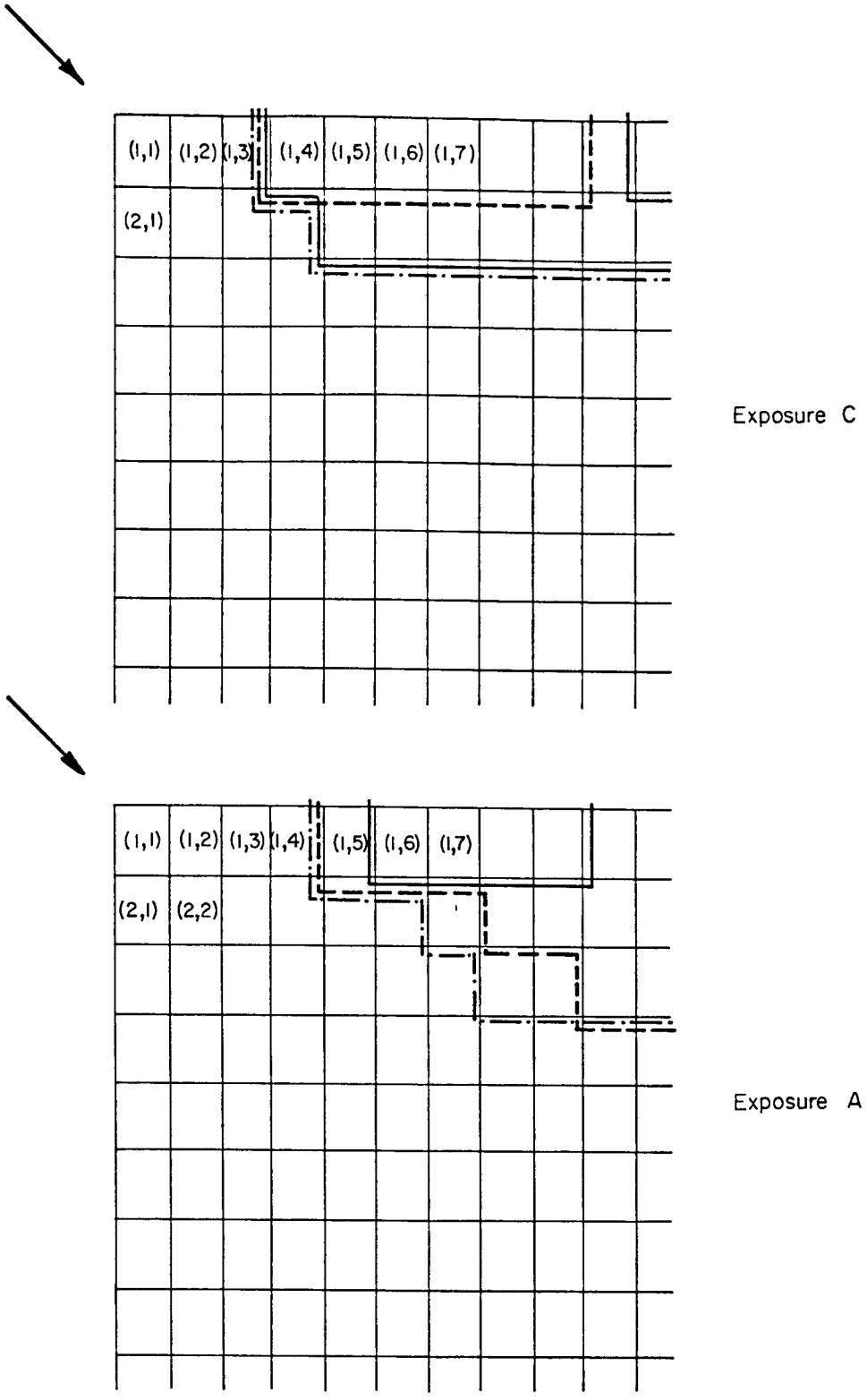


Figure 6. Three Typical Realizations of Paver Failure -- Original Configuration with Zero Height Parapet.

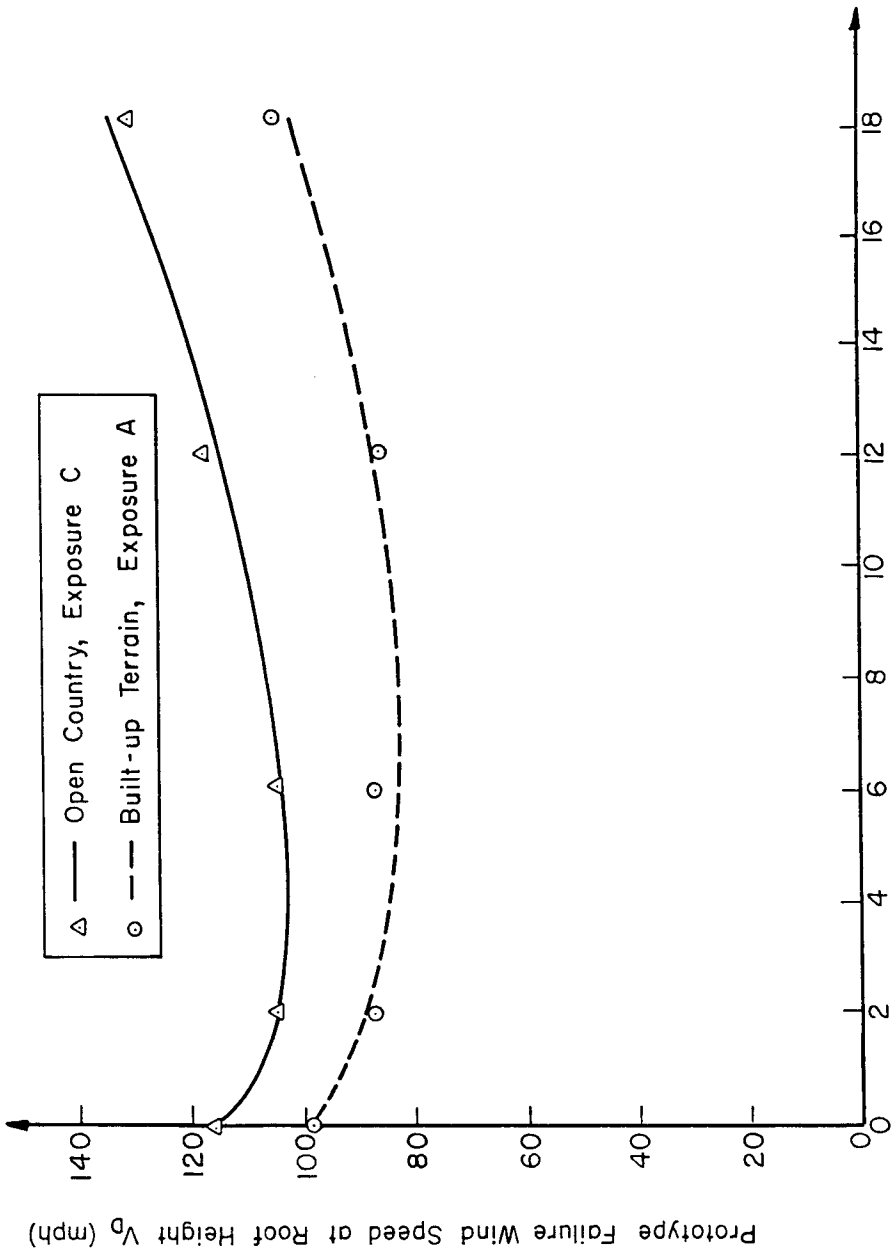


Figure 7. Failure Wind Speed at Roof Height -- Modified Paver Configuration

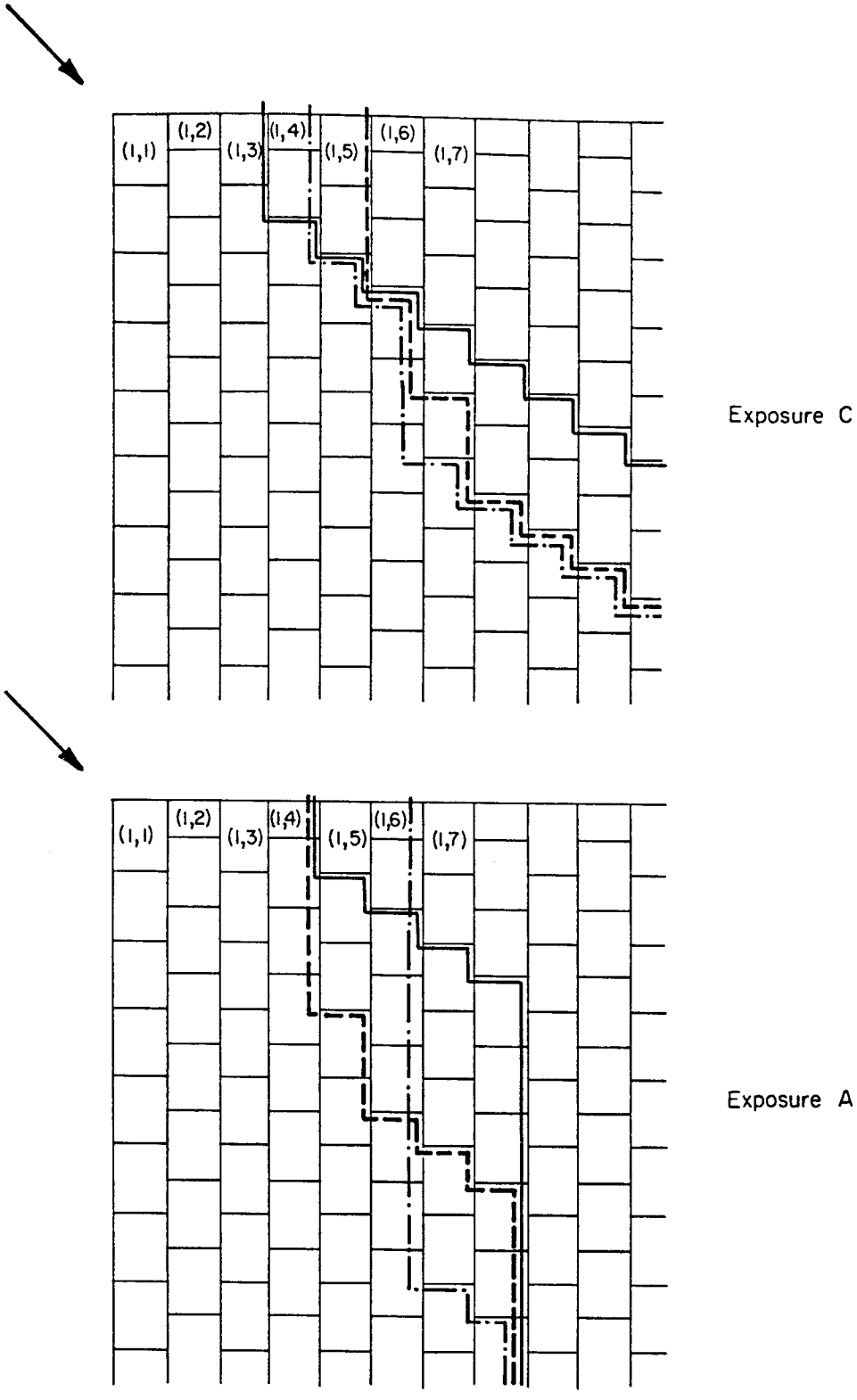


Figure 8. Three Typical Realizations of Paver Failure -- Modified Configuration with Zero Height Parapet.

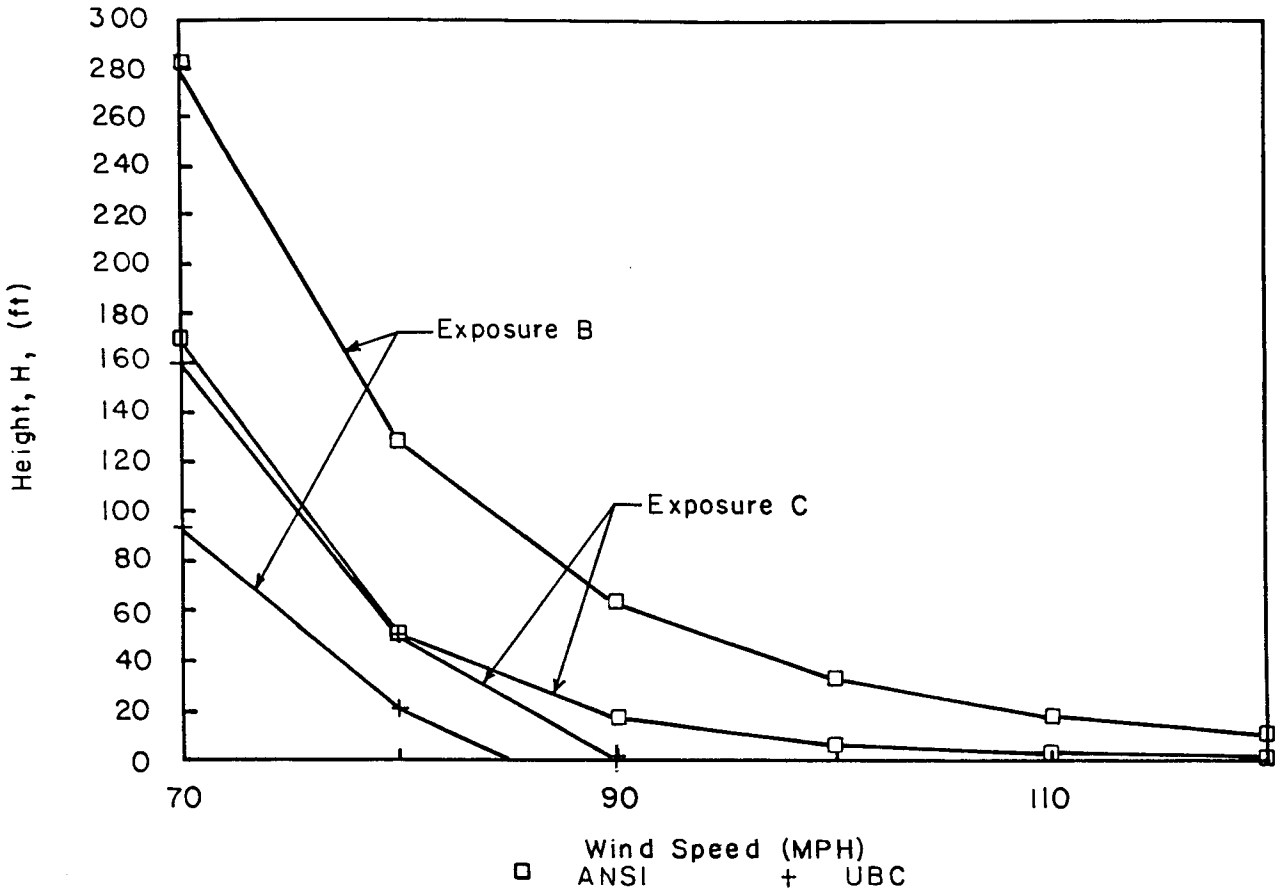


Figure 9. Maximum Building Height Estimated Using UBC and ANSI Standard -- Original Configuration with 12 in. Parapet, Exposure B.

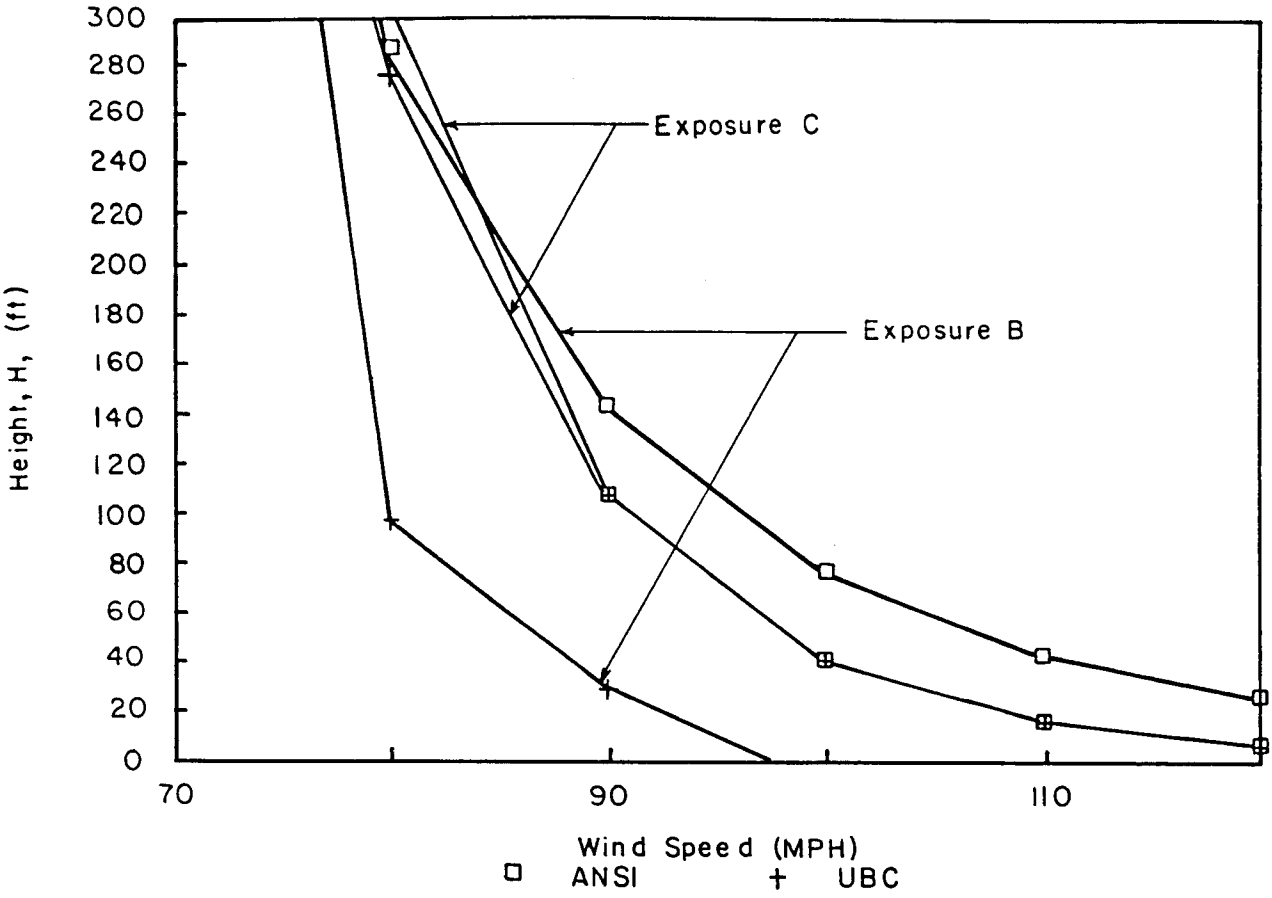


Figure 10. Maximum Building Height Estimated Usting UBC and ANSI Standard -- Modified Configuration With 12 in. Parapet, Exposure C.